Molecular Therapy
Nucleic Acids
Original Article

lncRNA SNHG1 Promotes Basal Bladder Cancer Invasion via Interaction with PP2A Catalytic Subunit and Induction of Autophagy

Jiheng Xu,[1] Rui Yang,[1] Xiaohui Hua,[1] Maowen Huang,[1] Zhongxian Tian,[1] Jingxia Li,[1] Hoi Yun Lam,[1] Guosong Jiang,[1] Mitchell Cohen,[1] and Chuanshu Huang[1]

[1]Department of Environmental Medicine, New York University School of Medicine, 341 East 25th Street, New York, NY 10010, USA

Although basal muscle-invasive bladder cancers (MIBCs) are predominant, are more aggressive, and have bad prognoses, molecular mechanisms underlying how basal MIBC formation/progression have been barely explored. In the present study, SNHG1, a long non-coding RNA, was shown to be expressed at higher levels in basal MIBC cells than in other types of bladder BC cells, and its presence could promote basal MIBC cell invasion. The results revealed that SNHG1 specifically induced MMP2 expression via increasing its transcription and mRNA stability. In one mechanism, SNHG1 directly bound with PP2A catalytic subunit (PP2A-c) to inhibit interactions of PP2A-c with c-Jun and then promoted c-Jun phosphorylation that, in turn, mediated *MMP2* transcription. In another mechanism, SNHG1 markedly induced autophagy in the cells via induction of increases in the abundance of autophagy-related proteins. The latter initiated autophagy and further abolished miR-34a stability, which reduced overall miR-34a binding directly to the 3′ UTR of *MMP2* mRNA, thereby promoting *MMP2* mRNA stabilization. These results provided novel insight into understanding the specific functions of SNHG1 in basal MIBC. Such findings may ultimately prove highly significant for the design/synthesis of new SNHG1-based compounds for the treatment of basal MIBC patients.

INTRODUCTION

Bladder cancer (BC) is one of the most common malignant urothelial tumors in the United States, with steadily rising incidence and high-risk recurrence.[1,2] It has been reported that muscle-invasive BC (MIBC) is characterized by rapid progression, metastasis, and an overall bad prognosis and poor survival rate.[3] Like breast cancer, MIBC is heterogeneous and can be divided into two groups, i.e., basal and luminal subtypes.[4] Basal MIBC has recently been shown to be the more aggressive type and is matched with lymph-node metastases and associated with a poorer survival rate.[5,6] Considering this, a better understanding of the molecular mechanisms of the invasive abilities of basal MIBC could contribute to the development of new therapeutics to help treat/prevent the increasing number of BCs.

Basal MIBC is thought to be characterized by some protein markers, including KRT5, KRT6, and KRT14.[7] However, the most recent report reveals that non-coding RNAs might be involved in molecular characterization of MIBC.[8,9] Long non-coding RNA (lncRNA) is a group of non-coding transcripts comprising >200 nt. The role of lncRNA in the pathogenesis of several human malignancies, including genitourinary cancers, has been receiving greater attention in the past few years.[10,11] Recent reports have revealed that dysregulated lncRNAs are involved in epithelial-to-mesenchymal transition (EMT) and metastasis in human BC. For example, high expression of the lncRNA *UCA1* promotes the invasion and EMT of BC,[12] and high LINC01605 expression predicts poor prognosis and promotes tumor progression.[13] Similarly, small nucleolar RNA host gene 1 (*SNHG1*), an lncRNA gene located in chromosome 11, is aberrantly expressed in many cancers, such as glioma, esophageal cancers, and gastric cancers.[14–16] SNHG1 has been reported to act as an oncogenic lncRNA in many other cancers by being involved in cancer proliferation, apoptosis, and metastasis.[17,18] For example, SNHG1 promotes invasion of hepatocellular carcinoma (HCC) by acting as a molecular sponge to modulate miR-195, and downregulation of lncRNA SNHG1 inhibits pancreatic cancer cell proliferation, metastasis, and invasion by suppressing the Notch-1 signaling pathway.[18,19] However, to date, the role of SNHG1 in basal MIBC has not been explored yet. The present study has identified that SNHG1-initiated autophagy mediated miR-34a degradation and, consequently, reduced miR-34a binding to the 3′ UTR of *MMP2* mRNA, therefore increasing *MMP2* mRNA stabilization and BC cell invasion.

RESULTS

lncRNA SNHG1 Overexpression Promoted Basal MIBC Cell Invasion by Targeting MMP2

To evaluate the potential involvement of lncRNA SNHG1 in different subtypes of human BC, six cell lines—RT4, RT112, HT1376, UMUC3, T24, and U5637—and one normal bladder cell line, UR-Otsa, were evaluated for SNHG1 expression. The results indicated

Received 10 March 2020; accepted 12 June 2020;
https://doi.org/10.1016/j.omtn.2020.06.010.

Correspondence: Chuanshu Huang, MD, PhD, Department of Environmental Medicine, New York University School of Medicine, 341 East 25th Street, New York, NY 10010, USA.
E-mail: chuanshu.huang@nyumc.org

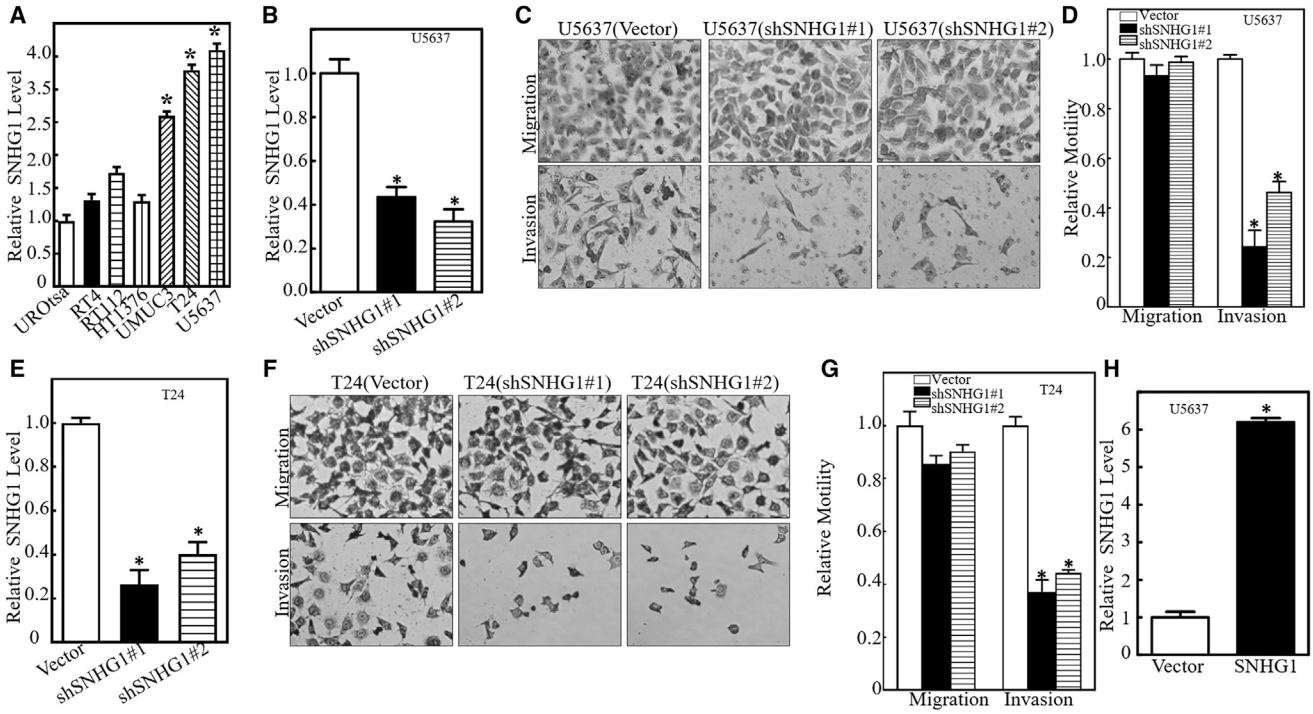

Figure 1. SNHG1 Was Required for Cancer Cell Invasion in Human Basal MIBC Cells

(A) SNHG1 levels in human BC cell lines (RT4, RT112, HT1376, UMUC3, T24, and U5637) were determined and compared with normal urothelial cell lines (UROtsa) using real-time PCR. *SNHG1* expression was normalized to *GAPDH* mRNA expression. *p = 0.0091 (significant difference). (B) Two shRNA-targeted SNHG1 and nonsense control vector plasmids were stably transfected into U5637 cells; stable transfectants were identified by real-time PCR. *p = 0.0084 (significant difference). (C and D) Invasion abilities of U5637(Vector), U5637(shSNHG1#1), and U5637(shSNHG1#2) cells were determined using Biocoat Matrigel invasion chambers. Migration ability was determined using an empty insert membrane without Matrigel. The migrated and invasive cells were photographed under an Olympus DP71 (C); and the number of the cells in each image was counted by the software "Image J." The invasion rate was normalized with the insert control according to the manufacturer's instruction; *p = 0.0088 (significant difference) (D). (E) Stable transfectants of T24(Vector), T24(shSNHG1#1), and T24(shSNHG1#2) were identified by real-time PCR; *GAPDH* was RNA loading control. *p = 0.0085 (significant difference). (F and G) Invasions and migrations of T24(Vector), T24(shSNHG1#1), and T24(shSNHG1#2) cells were were photographed under an Olympus DP71 (F); Invasion rates among T24(Vector), T24(shSNHG1#1), and T24(shSNHG1#2) cells were calculated as described above. *p = 0.0092 (significant difference) (G). (H) Identification of ectopic expression of SNHG1 and its scramble vector in U5637 cells. *p = 0.0004 (significant difference).

that SNHG1 expression in the three basal MIBC cell lines T24, U5637, and UMUC3, according to a previous report,[8] was much higher than in the other BC lines (Figure 1A). It has been known that basal MIBCs are aggressive and are associated with poor clinical outcomes.[20] To uncover the potential role of SNHG1 in basal MIBC, a small hairpin RNA (shRNA) specifically targeting human SNHG1 (shSNHG1) was stably transfected into U5637 and T24 human basal MIBC cells (Figures 1B and 1E). Knockdown of SNHG1 remarkably inhibited basal MIBC invasion in both U5637 and T24 cells (Figures 1C, 1D, 1F, and 1G). Furthermore, ectopic expression of SNHG1 led to a striking increase in U5637 cell invasion (Figures 2A and 2B). These results reveal that SNHG1 does play an essential role in human BC invasion.

To elucidate the potential mechanism underlying the SNHG1 upregulation of invasion, western blot analyses were performed to screen the cells for potential SNHG1 downstream invasion regulators. As shown in Figure 2C, knockdown of SNHG1 specifically inhibited MMP2 protein abundance but promoted or had no effect on other invasion-related factors, including RhoA, RhoC, XIAP, and Rho-GDIα. Consistently, ectopic expression of SNHG1 led to increased MMP2 expression in comparison to scramble vector transfectants (Figure 2D). Thus, it was anticipated here that MMP2 might be a SNHG1 downstream effector responsible for the promoting effect on invasion in human basal MIBC cells. To test this notion, shRNA specifically targeting MMP2 (shMMP2#1 and shMMP2#2) were stably transfected into U5637(SNHG1) cells (Figure 2E), and the effect on invasion was evaluated. The results showed that knockdown of MMP2 decreased the invasion of U5637(SNHG1) cells compared with that noted in scramble nonsense transfectants, while it did not affect U5637(SNHG1) migration under the same experimental conditions (Figures 2F and 2G). Given that many previous studies, from us[21,22] as well as from others,[23,24] showing that MMP2 is able to specifically promote invasion, rather than migration, in many cancer cells, and that MMP2 is a well-known proteinase essential for the breakdown of the extracellular matrix (EMC) in cancer cell invasion, our results reveal that MMP2 is at least a SNHG1 downstream effector specifically responsible for the promotion of human basal MIBC-invasive activities.

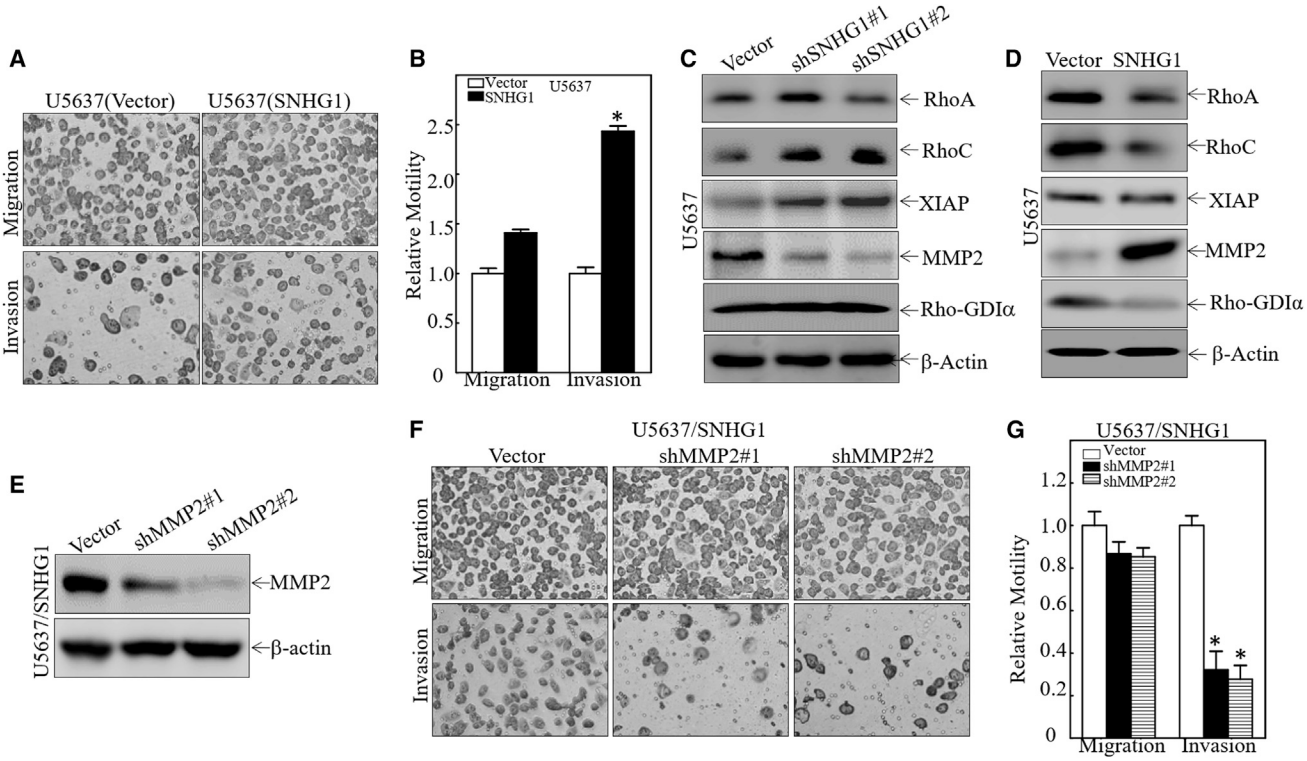

Figure 2. SNHG1-Induced MMP2 Overexpression Mediated Basal MIBC Cell Invasion

(A and B) Invasions of U5637(Vector) and U5637(SNHG1) cells were evaluated in a Transwell invasion assay. The migrated and invasive cells were photographed under an Olympus DP71 (A); Invasion rates between the cells were calculated as described above. *p = 0.0056 (significant difference) (B). (C and D) Indicated cell extracts were subjected to western blot to determine expression of RhoA, RhoC, XIAP, Rho-GDIα, and MMP2 proteins; β-actin was loading control. (E) MMP2 knockdown constructs were stably transfected into U5637(SNHG1) cells. The knockdown efficiency of MMP2 protein was assessed by western blotting. (F and G) U5637(SNHG1/MMP2#1) cells, U5637(SNHG1/MMP2#2) cells, and U5637(SNHG1/Vector) cells were subjected to evaluate invasion; The migrated and invasive cells were photographed under an Olympus DP71 (F); the invasion rate between the cells was calculated as described above. Results shown are means ± SD from triplicate experiments. *p = 0.0076 (significant difference) (G).

SNHG1 Promoted MMP2 Transcription by Increasing c-Jun Protein Phosphorylation

To investigate potential mechanisms underlying how SNHG1 upregulated MMP2 protein expression in the BC cells, *MMP2* mRNA levels were evaluated. The results showed that *MMP2* mRNA levels were markedly reduced in SNHG1 knockdown transfectants in comparison to that in scramble vector transfectants (Figure 3A). Consistently, ectopic expression of SNHG1 remarkably promoted *MMP2* mRNA levels (Figure 3B). To determine whether SNHG1 regulated MMP2 expression at the transcription level and/or its mRNA stability level, the wild-type (WT) *MMP2* promoter-driven luciferase reporter was transfected into U5637(Vector), U5637(shMMP2#1), and U5637(shMMP2#2) cells. The results showed that knockdown of SNHG1 inhibited *MMP2* promoter-driven reporter transcription activity in U5637 cells (Figure 3C). As expected, ectopic expression of SNHG1 remarkably enhanced MMP2 promoter activity in these same cells (Figure 3D). Next, to exclude the possibility of SNHG1 regulation of *MMP2* mRNA stability, mRNA stabilities were evaluated in presence of ActD to inhibit new mRNA synthesis in both U5637(Vector) and U5637(SNHG1) cells. Unexpectedly, upon inhibition of any new mRNA transcription due to the presence of ActD, *MMP2* mRNA degradation rates in U5637(SNHG1) cells were seen to be much slower than in the U5637(Vector) cells (Figure 3E). These results clearly show that SNHG1 upregulated MMP2 abundance in the cells via a promotion of both *MMP2* mRNA transcription and *MMP2* mRNA stability.

It has been reported that activation of nuclear factor κB (NF-κB), Sp1, and c-Jun can promote *MMP2* transcription.[25–27] Thus, the study here next evaluated the expression of these transcription factors in both SNHG1 overexpression cells and in their scramble vector transfectants. The results showed that SNHG1 overexpression specifically induced c-Jun phosphorylation, Sp1 showed no significant change, and NF-kB was only present at low levels (Figure 3F), suggesting that c-Jun might be the effector in SNHG1-mediated upregulation of MMP2 expression. To verify this, a dominant-negative mutant c-Jun (TAM67) was used to better clarify the role of c-Jun in SNHG1-induced MMP2 expression. Blocking c-Jun activation by ectopic expression of TAM67 did result in the inhibition of both MMP2 protein and mRNA expression (Figures 3G and 3H). Moreover, invasion was remarkably decreased in c-Jun dominant-negative

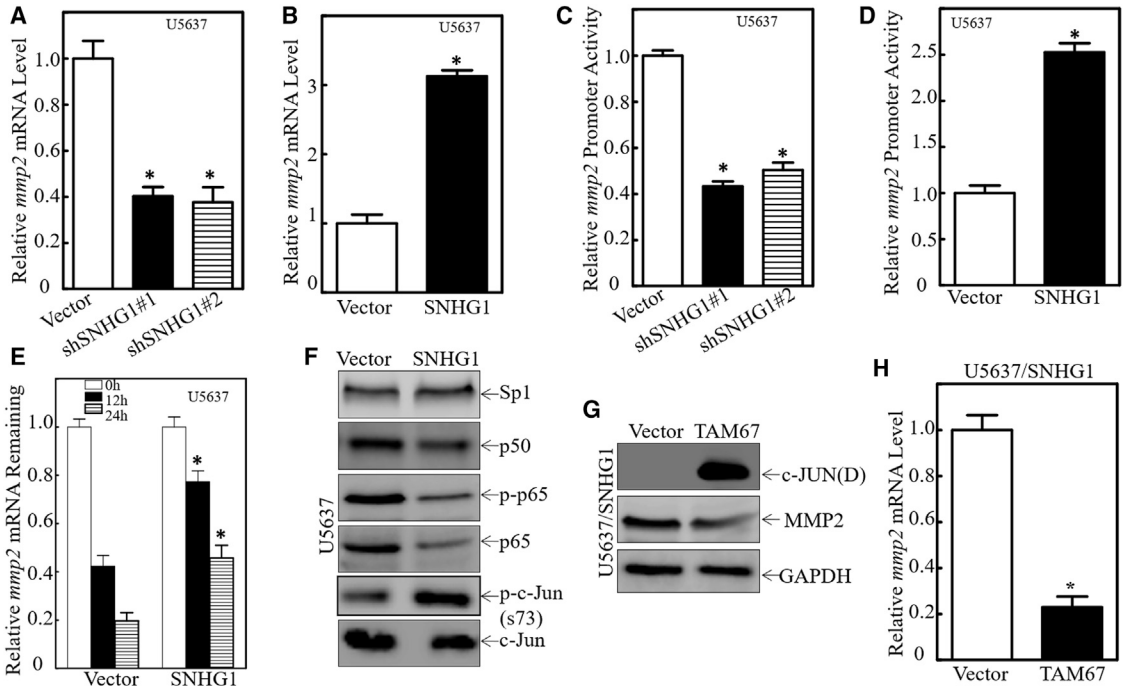

Figure 3. c-Jun Activation Mediated SNHG1-Promoted *MMP2* Transcription in Human Basal MIBC Cells

(A and B) *MMP2* mRNA levels were evaluated in indicated transfectants using real-time PCR; *GAPDH* was used as an internal control. *p = 0.0085 in (A), and *p = 0.0073 in (B) (significant difference). (C and D) Indicated cells were transfected with MMP2 promoter-driven luciferase reporter together with pRL-TK. Transfectants were seeded into 96-well plates and then subjected to determine MMP2 promoter activity by measuring luciferase activity. pRL-TK was used as an internal control to normalize transfection efficiency. *p = 0.0088 in (C), and *p = 0.0081 in (D) (significant difference). (E) Indicated cells were seeded into 6-well plates. After synchronization, cells were treated with Act D for indicated times. Total RNA was then isolated and subjected to real-time PCR analysis of *MMP2* mRNA levels; *GAPDH* was internal control. *p = 0.0095 (significant difference). (F) Indicated cell extracts underwent western blotting for determination of SP1, P50, p-P65, P65, p-c-Jun, and c-Jun expression. (G) TAM67 was stably transfected into U5637(SNHG1) cells, and the stable transfectants were then identified for c-Jun(D) (TAM67) expression and determination of MMP2; GAPDH was used as an internal control. (H) Indicated cells were extracted for total RNA with TRIzol. Real-time PCR was used to determine *MMP2* mRNA expression; *GAPDH* was used as an internal control. Results shown are means ± SD from at least triplicate experiments. *p = 0.0005 (significant difference).

mutant overexpressed U5637(SNHG1) transfectants (Figures 4A and 4B). Collectively, these results demonstrate that phosphorylated c-Jun is a critical transcription factor mediating SNHG1 promotion of basal MIBC cell invasion, in part, by enhancing MMP2 transcription.

SNHG1 Was Able to Directly Bind to Phosphatase PP2A Catalytic Subunit (PP2A-c), Attenuating Interactions of PP2A-c with c-Jun and Leading to c-Jun Activation

Protein phosphatase is a common enzyme that removes phosphate groups from phosphorylated amino-acid residues on proteins.[28] To evaluate whether SNHG1 could have an impact on phosphatases in the cells, the c-Jun upstream potential protein phosphatases, including PP2A-c and its phosphorylated versions, PHLPP1 and PHLPP2, were evaluated in the cell lines. The results showed that, as a result of SNHG1 overexpression, only phosphorylated PP2A-c (p-PP2A-c) was found to be present at a very high level, while the others showed no significant differences or a slight downregulation in expression from levels in the U5637(Vector) cells (Figure 4C). It was of note that p-PP2A-c inhibited phosphatase activity and PP2A-c can directly interact with c-Jun to decrease c-Jun phosphorylation.[29] To better understand how SNHG1 could regulate PP2A-c phosphorylation, RNA immunoprecipitation (RIP) assays were performed. The results showed that PP2A-c exhibited a strong interaction with SNHG1 (Figure 4D). More interesting was the finding that ectopic expression of SNHG1 inhibited the interactions between PP2A-c and c-Jun (Figure 4E). These results indicate that SNHG1 overexpression leads to its binding to PP2A-C, in turn, reducing PP2A-C interaction with c-Jun, which further results in increased c-Jun phosphorylation and activation.

SNHG1 Maintained *MMP2* mRNA Stabilization by Reducing miR-34a Expression

Given that microRNAs (miRNAs) have been reported to regulate mRNA degradation by targeting the bound mRNA 3′ UTR[30] and our aforementioned results showing that SNHG1 overexpression could stabilize *MMP2* mRNA (Figure 3E), this study next evaluated the potential effect of SNHG1 on *MMP2* mRNA 3′ UTR activity. The results indicated that ectopic expression of SNHG1 promoted *MMP2* mRNA 3′ UTR activity (Figure 5A). A bioinformatics search for putative miRNAs that could potentially target this *MMP2* mRNA 3′ UTR was performed using the TargetScan database, and the results are shown in Table 1. Expression of these miRNAs was then

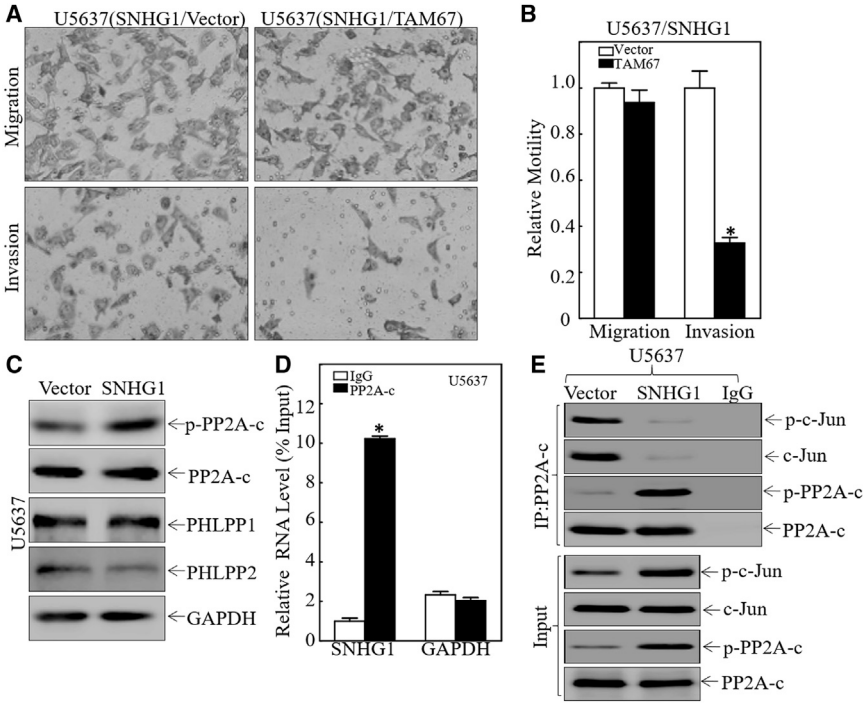

Figure 4. C-Jun Activation Was Induced by SNHG1 through Its Interaction with PP2A-c and, in Turn, Was Responsible for SNHG1 Mediation of Invasion in Human Basal MIBC Cells

(A and B) U5637(SNHG1/Vector) cells and U5637(SNHG1/TAM67) cells were evaluated in a Transwell invasion assay (A). Invasion rates between them were normalized to insert control according to manufacturer's instructions (B). *p = 0.0062 (significant difference). (C) Indicated cell extracts underwent western blots for determination of p-PP2A, PP2A-c, PHLPP1, and PHLPP2 protein expression. GAPDH was used as an internal control. (D) RNA-IP was carried out to evaluate specific interaction of SNHG1 with PP2A-c. GAPDH was used as a negative control. *p = 0.0003 (significant difference). (E) The co-IP of c-Jun with anti-PP2A-c antibodies were performed in U5637(Vector) and U5637(SNHG1) cells.

determined in both U5637(Vector) and U5637(SNHG1) cells; expression of miR-34a was seen to be significantly decreased in U5637(SNHG1) cells, while other miRNAs did not show any significant downregulation (Figure 5B). To test whether miR-34a was able to directly bind to the 3′ UTR of *MMP2* mRNA so as to cause destabilization, a mutation of the miR-34a binding site in the 3′ UTR of *MMP2* mRNA luciferase reporter was constructed (Figure 5C). The WT and mutant *MMP2* 3′ UTR luciferase reporters were then transiently transfected into U5637(SNHG1) and scramble vector cells together with pRL-TK. The results showed that the 3′ UTR of *MMP2* mRNA luciferase activity was significantly increased in U5637(SNHG1) cells compared with that in U5637(Vector) cells, whereas the mutant *MMP2* 3′ UTR luciferase reporter completely attenuated the U5637 cell responses to SNHG1 overexpression (Figure 5D), suggesting that the miR-34a binding site is required for SNHG1 promoting MMP2 mRNA 3′ UTR activity.

To determine the role of miR-34a in SNHG1 regulation of MMP2 expression, a miR-34a-overexpressing construct was stably transfected into U5637(SNHG1) cells, and the stable transfectant was identified (Figure 5E). Ectopic expression of miR-34a markedly promoted *MMP2* mRNA degradation (Figure 5F), and in turn, resulting in inhibition of MMP2 protein expression (Figure 5G). As expected, ectopic expression of miR-34a reversed the promotion of invasion due to SNHG1 overexpression in the U5637 cells (Figures 5H and 5I). Taken together, these results demonstrate that SNHG1 overexpression inhibits miR-34a expression, results in its having less impact on the *MMP2* mRNA 3′ UTR, and further leads to *MMP2* mRNA stabilization, therefore promoting human basal MIBC cell invasion.

SNHG1 Enhanced miR-34a Degradation through Autophagy

To elucidate potential mechanisms underlying SNHG1-related reductions in miR-34a expression, miR-34a stability in U5637(SNHG1) cells compared with those in U5637(Vector) cells was evaluated. Upon inhibition of new RNA transcription with Actinomycin D (Act D), miR-34a degradation rates in U5637(SNHG1) cells were much higher than those in U5637(Vector) cells (Figure 6A), suggesting that SNHG1 overexpression promotes miR-34a degradation in basal MIBC cells.

It has been reported that miRNA degradation could also be induced by autophagy.[31,32] To evaluate the potential involvement of autophagic responses in the degradation of miR-34a due to SNHG1 overexpression in U5637 cells, expression of different autophagy regulators and the conversion rate of LC3 I to LC3 II following ectopic expression of SNHG1 were measured. The results indicated that SNHG1 overexpression led to substantial conversion of LC3 I to LC3 II and total LC3 I expression. In addition, not only ATG3 and ATG7 expression but also the conjunction rate between ATG5 and ATG12, which reflects autophagy flux, was much higher in U5637(SNHG1) cells than in U5637(Vector) cells (Figure 6B), revealing that SNHG1 overexpression might induce autophagic responses in human basal MIBC U5637 cells. Further, a tandem mcherry-LC3B fusion expression construct was stably transfected into U5637(Vector) and U5637(SNHG1) cells to monitor autophagosome formation. Using confocal laser scanning microscopy, as shown in Figures 6C and 6D, SNHG1-induced formation of autophagosomes and mcherry-LC3B puncta formation were significantly increased after treatment with the autophagy inhibitor bafilomycin A1 (BAF). These results provide strong evidence indicating autophagic induction by SNHG1 overexpression. Of note, miR-34a expression and stability were restored upon treatment of the U5637(SNHG1) cells with BAF treatment (Figures 6E and 6F).

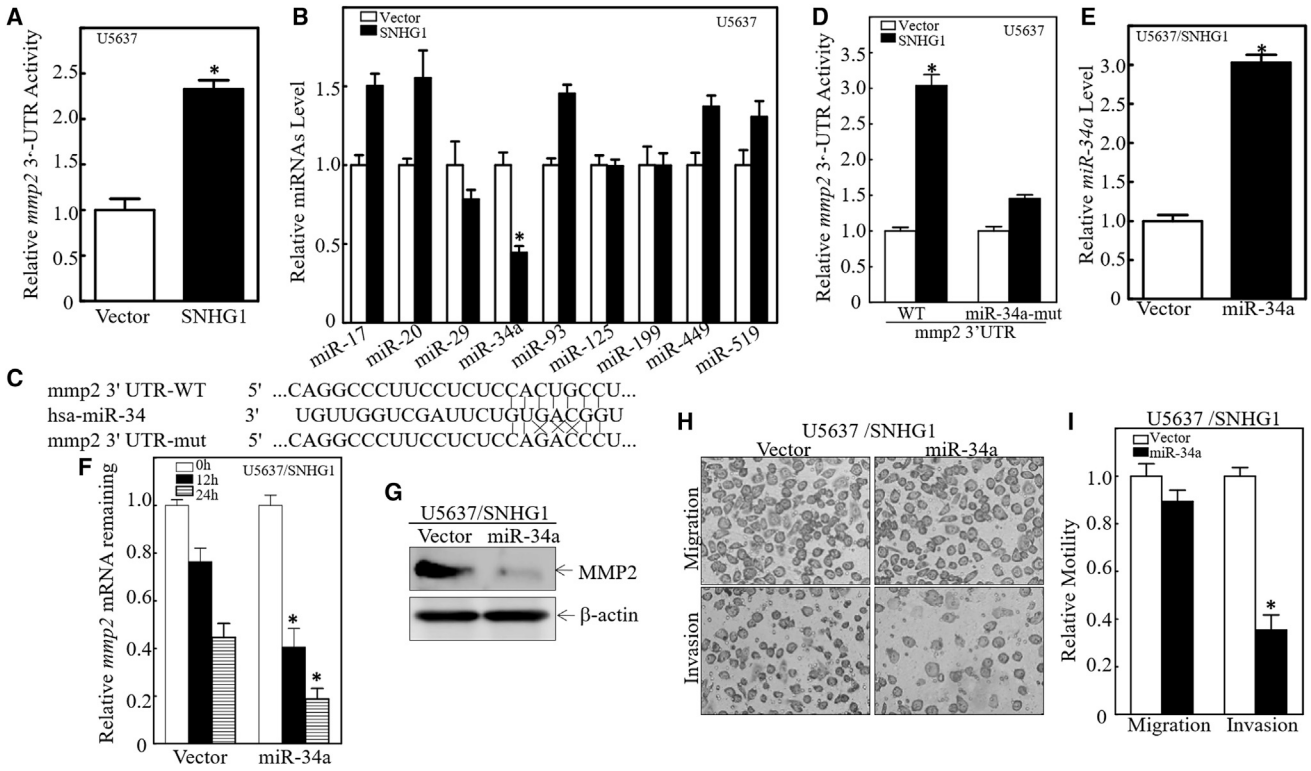

Figure 5. miR-34a Downregulation Was Crucial for SNHG1-Mediated *MMP2* mRNA Stabilization and Invasion in Basal MIBC Cells

(A) An MMP2 mRNA 3′ UTR luciferase reporter was transiently transfected into the indicated cells, and the luciferase activity of each transfectant was evaluated. Luciferase activity is presented as relative to vector transfectant with normalization to internal transfection control pRL-TK. *p = 0.0083 (significant difference). (B) Quantitative real-time PCR was used to determine expression of miRNA in indicated cells. *p = 0.0091 (significant difference). (C) Schematic of construction of the MMP2 mRNA 3′ UTR luciferase reporter and its mutants were aligned with miR-34a. (D) WT and mutant MMP2 mRNA 3′ UTR luciferase reporters were transiently co-transfected with pRL-TK into indicated cells. Luciferase activity of each transfectant was evaluated; results are presented as relative MMP2 mRNA 3′ UTR activity. *p = 0.0063 (significant difference). (E) miR-34a constitutively expressed plasmids were stably transfected into U5637(SNHG1) cells. Stable transfectants were identified by real-time PCR. *p = 0.0065 (significant difference). (F) U5637(SNHG1/miR-34a) cells and their scramble vector transfectant were seeded into 6-well plates. After synchronization, cells were treated with Act D for indicated times. Total RNA was isolated and subjected to quantitative real-time PCR analysis for *MMP2* mRNA levels; *GAPDH* was used as internal control. *p = 0.0082 (significant difference) (G) Cell lysates extracted from indicated cells were evaluated by western blots to determine MMP2 protein expression; β-actin was loading control. (H and I) U5637(SNHG1/Vector) cells versus U5637(SNHG1/miR-34a) cells were evaluated in a Transwell invasion assay (H); invasion rate between them was normalized to insert control according to the manufacturer's instructions (I). Results shown are means ± SD from at least triplicate experiments. *p = 0.0074 (significant difference).

Consistent with the results obtained from the *in vitro* cell-culture model, miR-34a expression was significantly decreased, while *MMP2* mRNA was greatly upregulated in human BC tissues as compared to that in their corresponding adjacent normal bladder tissues (Figures 7A and 7B). Moreover, the relationship between miR-34a expression and its regulated *MMP2* mRNA levels in the same 23 pairs of human BC tissues and matched adjacent normal bladder tissues was also evaluated. The correlation analyses of miR-34a and *MMP2* mRNA levels in these tissues indicated that there was a negative pathophysiological association between miR-34a and *MMP2* mRNA levels (Figure 7C). Collectively, the results obtained from current studies demonstrate that, on one hand, SNHG1 overexpression increases its binding to PP2A-C protein, by which it reduces PP2A-C de-phosphorylation of c-Jun, thereby leading to c-Jun activation and its regulated MMP2 mRNA transcription; on other hand, SNHG1 also induces autophagy, which leads to miR-34a degradation, and, in turn, reducing its interaction with *MMP2* mRNA and attenuating *MMP2 mRNA* degradation. The aforementioned induction of *MMP2* mRNA transcription and reduction of *MMP2* mRNA degradation coordinately leads to MMP2 expression and further BC invasion, as illustrated in Figure 7D.

DISCUSSION

MIBCs have been characterized by their rapid progression, high metastatic potentials, and poor prognoses. As such, MIBCs have been an important challenge for urologists and scientists for several decades.[33] MIBCs are heterogeneous and can be divided into basal and luminal subtypes that are highly reminiscent of those found in breast cancers.[34] Focusing on the molecular subtypes of MIBC represents a promising approach to help potentially stratify patients for neoadjuvant treatments.[5,35] The basal MIBC subtype is more intrinsically aggressive than the luminal subtype, suggesting that the former has

Table 1. The Potential miRNA Binding Sites in the mmp2 mRNA 3′ UTR Region

Position 515-521 of mmp2 3' UTR	5' ...CAGUUUGCUUUGUAUGCACUUUG...
hsa-miR-17	3' GAUGGACGUGACAUUCGUGAAAC ...
Position 515-521 of mmp2 3' UTR	5' ...CAGUUUGCUUUGUAUGCACUUUG...
hsa-miR-20	3' GAUGGACGUGAUAUUCGUGAAAU
Position 299-305 of mmp2 3' UTR	5' ...UGCUUUGGGCUGCCCUGGUGCUG...
hsa-miR-29	3' AUUGGCUAAAGUCUACCACGAU
Position 33-39 of mmp2 3' UTR	5' ...CAGGCCCUUCCUCUCCACUGCCU...
hsa-miR-34	3' UGUUGGUCGAUUCUGUGACGGU
Position 515-521 of mmp2 3' UTR	5' ...CAGUUUGCUUUGUAUGCACUUUG...
hsa-miR-93	3' GAUGGACGUGCUUGUCGUGAAAC
Position 952-959 of mmp2 3' UTR	5' ...AAACAGCAAGAGAACCUCAGGGA...
hsa-miR-125	3' AGUGUCCAAUUUCCCAGAGUCCCU
Position 682-688 of mmp2 3' UTR	5' ...ACCGAGUCUCUUCUCCACUGGAU...
hsa-miR-199	CUUGUCUAUCAGAUUU------GUGACCC
Position 33-39 of mmp2 3' UTR	5' ...CAGGCCCUUCCUCUCCACUGCCU...
hsa-miR-449	3' UGGUCGAUUGUUAUGUGACGGU
Position 515-521 of mmp2 3' UTR	5' ...CAGUUUGCUUUGUAUGCACUUUG...
hsa-miR-519	3' GUGAGAUUUCCCUCCGUGAAAC

more metastasis-related molecular mechanisms than the latter.[36] There are many studies concentrating on the aberrant expression of specific proteins in basal MIBC, such as KRT5, KRT14, and CD44.[37,38] lncRNAs are a heterogeneous group of non-coding transcripts longer than 200 nt, which have emerged as key players in fundamental biological processes, including tumorigenesis.[39–41] Abnormal expression of many lncRNAs affects cancer predisposition, development, and progression.[42] For example, we recently showed that nickel exposure causes hypermethylation of the MEG3 promoter and, hence, reduced expression of MEG3 lncRNA and resultant decrease in malignant transformation of human bronchial epithelial cells.[43] SNHG1 is a lncRNA, encoded by a gene of 11 exons and located at 11q12.3. The information about the biological function(s) of SNHG1 and its role in cancer is limited to HCC,[44,45] lung cancer,[46] and prostate cancer.[47] In HCCs, overexpression of SNHG1 contributes to HCC proliferation, invasion, and migration *in vitro* through the inhibition of miR-195.[45] SNHG1 promotes cell proliferation in prostate cancer by increasing CDK7 expression by competitively binding miR-199a-3p, while in lung cancer the mechanisms of growth induction by SNHG1 remains unknown.[47] The results from our most recent lncRNA deep-sequencing analysis using the Illumina HiSeqTM2000/2500 high-throughput platform to evaluate 5,929 known lncRNAs and 551,711 candidate lncRNAs found that the bladder-specific carcinogen *N*-butyl-*N*-(4-hydroxybutyl)-nitrosamine (BBN) treatment changed levels of 23 lncRNAs in mouse bladder epithelium. Real-time PCR verification of the abundances of lncRNAs and gain-function (overexpression) analyses identified SNHG1 as a key lncRNA candidate that may drive the formation of basal MIBCs in BBN-exposed mice. We discover that BBN induction of SNHG1 occurs in a time-dependent manner. Notably, RNA-sequencing data from a cohort (starBase v.2.0) comprising 533 human bladder samples (483 BC and 50 normal; grade/stage information unavailable) also show a remarkable increase of SNHG1 expression in BCs than in normal samples. Our current studies found that ectopic expression of SNHG1 in human basal MIBC cells promoted invasion. Their results, together with our other most recent findings showing that SNHG1 overexpression promotes normal urothelial cell transformation and growth, reveal our discovery that SNHG1 could completely mimic the biological effects of bladder carcinogen BBN exposure in terms of induction of urothelial cell transformation, invasion, and autophagy, as well as upregulation of ATG7 and MMP2 in human BC cells.[48,49] The results also showed that SNHG1 was significantly upregulated in human basal BC cells, and mechanistic studies showed that SNHG1 increased MMP2 expression via increases in the latter's mRNA transcription and stability.

With regard to *MMP2* mRNA transcription, SNHG1 could promote c-Jun phosphorylation by binding with PP2A-c, in turn, weakening the interactions of PP2A-c with c-Jun and, thus, resulting in increased *MMP2* transcription via c-Jun activation. In addition, SNHG1 could induce autophagy via upregulation of autophagy-related proteins and accelerating autophagy flux. This could then promote miR-34a autophagic degradation, consequently stabilizing *MMP2* mRNA. Evidence from clinical samples was consistent with these oncogenic

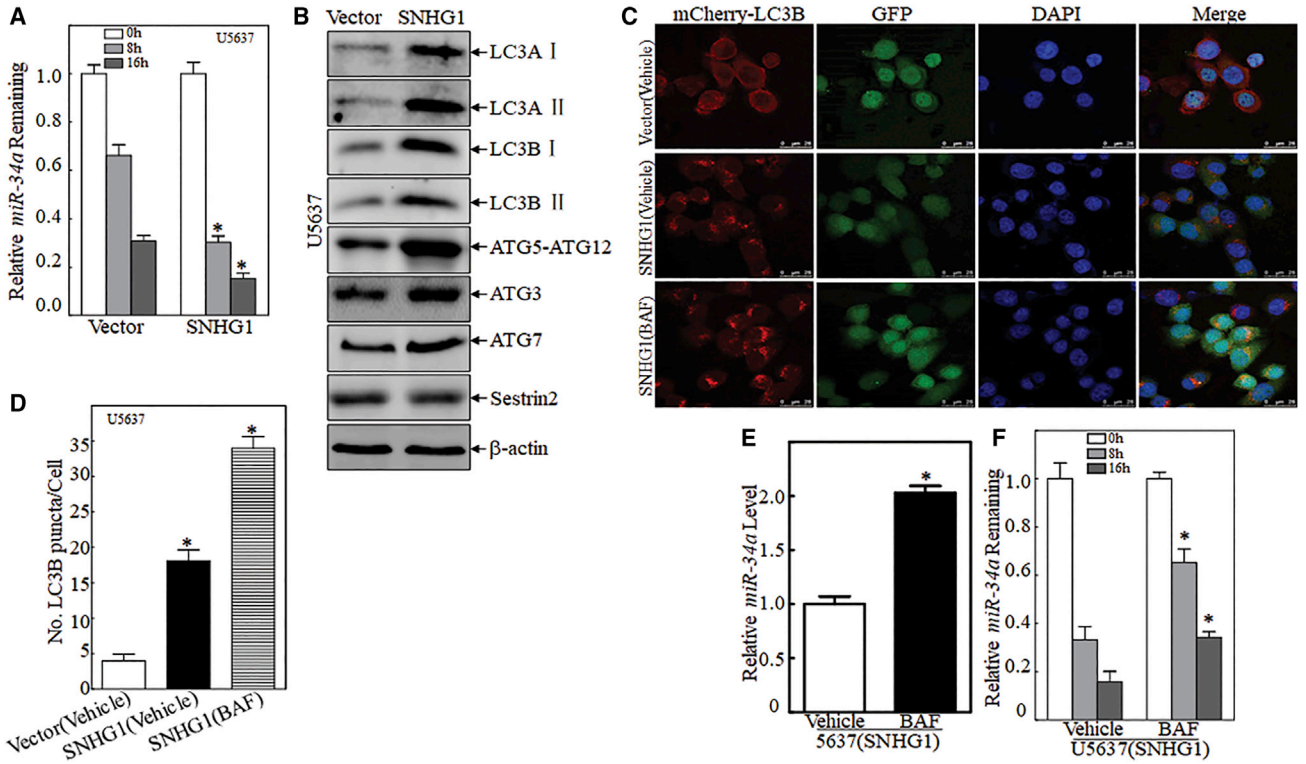

Figure 6. SNHG1 Overexpression Promoted miR-34a Degradation through Autophagy

(A) U5637(SNHG1) cells and their scramble vector transfectant were seeded into 6-well plates. After synchronization, cells were treated with Act D for indicated times. Total RNA was isolated and subjected to quantitative real-time PCR analysis for miR-34a levels; U6 was used as internal control. *p = 0.0062 (significant difference). (B) Indicated cell lysates were evaluated by western blot to determine expression of SESN2, ATG5/ATG12, ATG3, ATG7, LC3A, and LC3B proteins. (C) U5637(Vector) and U5637(SNHG1) cells were transfected with a mCherry-LC3B construct, and transfectants were treated with or without 2 nM BAF for 12 h. Representative images of mCherry-LC3B puncta were captured by using a confocal fluorescence microscope. (D) Number of puncta per mCherry-LC3B$^+$ cells were calculated/presented as described in Materials and Methods. *p = 0.0005 (significant difference). (E) Quantitative real-time PCR was used to determine expression of miR-34a in U5637 (SNHG1) cells treated with or without 2 nM BAF for 12 h. *p = 0.0085 (significant difference). (F) U5637(SNHG1) cells were incubated with Act D for indicated times with or without BAF. Total RNA was isolated, and quantitative real-time PCR performed to determine miR-34a levels. Fold change was normalized to internal control U6. Results shown are means ± SD from at least triplicate experiments. *p = 0.0093 (significant difference).

pathway findings. These results strongly supported the notion that SNHG1 might be acting as an oncogenic driver for basal MIBC development and also represents a potential therapeutic target in the management of basal MIBC patients.

Cancer metastasis involves multiple steps.[23] Stromal invasion is one of the most important steps, with destruction of the basement membrane playing a vital role for cancer cell invasion.[50] Matrix metalloproteinases (MMPs), a family of zinc-dependent proteolytic enzymes, are structurally and functionally related and are capable of degrading the ECM, thereby promoting cancer cell invasion and metastasis.[51] MMP2, a member of the MMP family, primarily hydrolyzes type IV collagen, the major structural component of the basement membrane;[52] therefore, MMP2 plays an essential role in promoting cancer cell invasion without affecting cell migration, as demonstrated in many previous studies.[53–56] Our previous studies and many other studies have proved that MMP2 could enhance MIBC invasion.[57,58] However, the mechanism of maintenance of MMP2 abundance is still unclear in the basal MIBC. Based on the results obtained from studies here, overexpression of SNHG1 significantly increased MMP2 protein levels, leading to enhanced basal MIBC cell-invasive activities. Interestingly, it was also seen that MMP2 abundance was regulated by SNHG1 via two different levels and pathways, i.e., impacts on *MMP2* mRNA transcription and stability.

Many transcription factors are overexpressed and activated in BC tissues. For example, c-Jun aberrant activation has been reported to play an important role in the regulation of cellular invasion.[59] Protein Phosphatase 2A (PP2A) is a serine/threonine phosphatase comprising a scaffolding subunit (PP2A-a), a catalytic subunit (PP2A-c), and a regulatory subunit (PP2A-b) and is always functionally impaired in cancer.[60] Previously, we found that PP2A could directly interact with c-Jun to inhibit c-Jun phosphorylation.[29] In the study reported here, it was seen that SNHG1 enhanced *MMP2* transcription via upregulation of c-Jun phosphorylation. It was also shown that SNHG1 positively regulated c-Jun activation by binding directly to PP2A-c, leading to

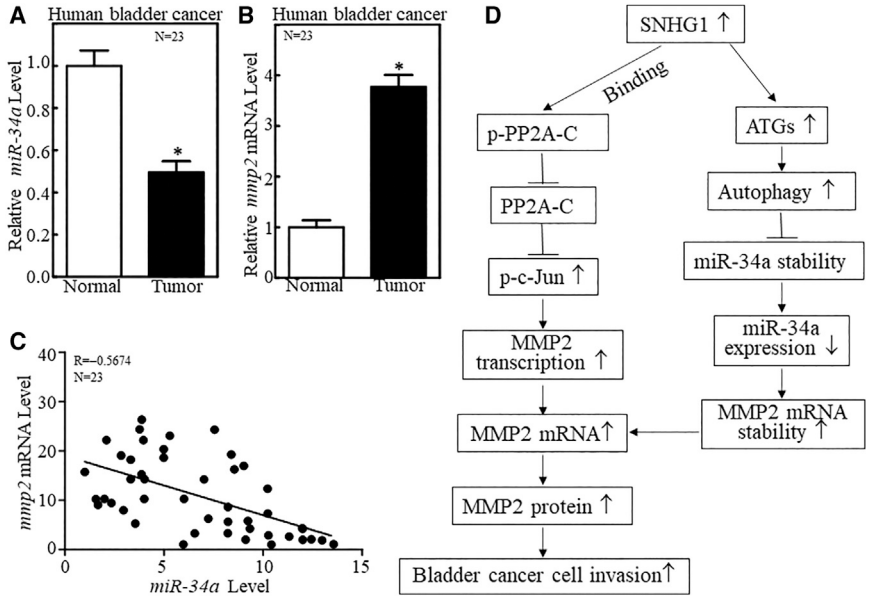

Figure 7. miR-34a Was Downregulated in Human MIBCs and Negatively Correlated with Overexpressed *MMP2* mRNA in BC Samples

(A and B) Total RNA lysates were prepared from human normal (N) and paired cancerous (T) tissues among 46 patients diagnosed with BC and subjected to quantitative real-time PCR analyses to determine levels of miR-34a (A) and *MMP2* mRNA (B). *p = 0.0092 (significant difference) in (A). *p = 0.0061 (significant difference) in (B). (C) Correlation analysis of pathophysiological association between miR-34a and *MMP2* mRNA in human BC tissues. Results shown are means ± SD from at least triplicate experiments. *p = 0.0084 (significant difference). (D) Schematic summary of molecular mechanisms underlying potential SNHG1 ability to impact on basal MIBC cell invasion.

increased PP2A-c phosphorylation and weakened interactions by PP2A-c and c-Jun. Thus, a highly specific and stable axis formed by SNHG1 together with PP2A-c resulted in SNHG1 promotion of c-Jun phosphorylation. To our knowledge, this is the first report of cross-talk between SNHG1 and a phosphatase by their interaction, as well as their co-regulation of *MMP2* mRNA transcription.

miRNAs are a class of small non-coding RNAs (≈19–25 nt) that play important roles in tumorigenesis; dysregulation of the expression of various miRNAs has been seen to be related to changes in metastatic potentials of several human cancers.[61] The biological function of miRNAs is mediated by their directly binding to mRNA 3′ UTR or 5′ UTR, resulting in modulation of their targeted mRNA instability or protein translation.[62,63] Our most recent studies have shown that p27 exerts a negative regulatory effect on miR-6981 expression by promoting the autophagy-mediated degradation and, in turn, releasing miR-6981 binding to the 5′ UTR of *PHLPP1* mRNA, therefore resulting in the upregulation of PHLPP1 protein translation.[32] miR-34a is downregulated and functions as a tumor suppressor in several types of human cancers.[64–67] For example, miR-34a is reported to inhibit retinoblastoma proliferation.[64] It is also believed that miR-34a could be a key regulator in the hallmarks of renal cell carcinoma.[65] miR-34a overexpression is able to contribute to the fate of gastric carcinogenesis and to inhibit the development of lung cancer.[66,67] Even so, to date, any role of miR-34a in the regulation of basal MIBC and associated mechanisms of effect is not known. In the present study, it was seen that miR-34a was significantly downregulated in human BC tissues as compared to that in corresponding adjacent normal bladder tissues; in comparison, *MMP2* mRNA levels showed an opposite expression pattern in the same human tissues. Statistically, miR-34a showed a negative correlation with *MMP2* mRNA expression in the tissues examined here. Moreover, it was also found that miR-34a overexpression was able to inhibit MMP2 expression and reverse the promotion of invasion due to SNHG1 overexpression in U5637 cells via miR-34a binding to the 3′ UTR region of *MMP2* mRNA. These results reveal a novel mechanism underlying the tumor-suppressive function of miR-34a in human basal MIBC.

The current studies also showed that SNHG1 significantly promoted autophagy-related ATG3 and ATG7 protein expression and accelerated autophagy flux; this subsequently induced miR-34a degradation after autophagy activation in the basal MIBC cells. This indicates that SNHG1 exhibits its oncogenic activity in human basal MIBC cells, most likely through a retardation of miR-34a stability. Further elucidation of the molecular mechanisms underlying SNHG1-mediated, autophagy-related protein expression will provide significant insight into understanding the action of this oncogenic lncRNA SNHG1 in human basal MIBC.

In conclusion, this study demonstrated that SNHG1 was upregulated in human basal MIBC cells and could promote basal MIBC cell-invasive capacities by increasing MMP2 expression through two different signaling pathways. One was that SNHG1 directly bound with PP2A-c to weaken the interaction of PP2A-c with c-Jun, leading to c-Jun phosphorylation and, in turn, promoting MMP2 mRNA transcriptional activation. The other one was that SNHG1 induced autophagy by upregulating autophagy-related protein expression and accelerating autophagy flux; such effect resulted in miR-34a autophagic degradation, an outcome that consequently reinforced *MMP2* mRNA stability. Taken together, the results here indicate that SNHG1 acts as an oncogenic lncRNA, which further strongly suggests that SNHG1 might serve as a potential therapeutic target in human basal MIBC therapy.

MATERIALS AND METHODS

Plasmids and Reagents

The shRNA constructs specific to MMP2 (shMMP2) and its scramble nonsense control construct were purchased from Open Biosystem

(Pittsburgh, PA, USA). The c-Jun dominant-negative mutant (PRC-CMV/TAM67) was described in our previous studies.[62] The shRNA constructs specifically targeting SNHG1 (shSNHG1s) were subcloned into a p-GIPZ vector. The full-length *Homo sapiens* SNHG1 sequences were synthesized and inserted downstream of the ZsGreen (Zoanthus sp. green fluorescent protein) gene of pmR-ZsGreen1 (Takara Bio, Otsu, Shiga, Japan). The miR-34a overexpression construct and mcherry-LC3B were obtained from Addgene (Cambridge, MA, USA). The human MMP-2 promoter luciferase was a generous gift from Dr. Yi Sun (University of Michigan, Ann Arbor, MI, USA). The 3′ UTR of *MMP2* mRNA was cloned into a p-MIR luciferase reporter vector. Plasmids were prepared using the Plasmid Preparation/Extraction Maxi Kit from QIAGEN (Valencia, CA, USA).

Antibodies specific against RhoA (2117S), RhoC (3430S), p-c-Jun Ser73 (3270S), total c-Jun (9165S), total P65 (4764S), p-P65 S536 (3033S), P50 (13681S), LC3A (4599S), LC3B(2775S), GAPDH (5174S), Atg5 (12994S), Atg3 (3415S), Atg7 (8558P), and PP2A-c (2259S) were purchased from Cell Signaling Technology (Beverly, MA, USA). The antibodies specific for RhoGDIα (sc-360), Sp1 (sc-H225), MMP-2 (sc-13594), and SESN2 (sc-292558) were purchased from Santa Cruz Biotechnology (Santa Cruz, CA, USA). Anti-XIAP (610763) antibody was obtained from BD Biosciences (Bedford, MA, USA). The antibody specific for ACTB (A5441) was purchased from Sigma (St. Louis, MO, USA). Specific antibodies against PHLPP1 and PHLPP2 were purchased from Bethyl Laboratories (Montgomery, TX, USA). Bafilomycin A1 (sc-201550) was purchased from Santa Cruz Biotechnology; actinomycin D (Act D) (50-76-0) was purchased from Fisher Scientific (Pittsburgh, PA, USA).

Cell Lines and Transfection

The normal urinary epithelial cell line UROtsa and different genetic background human BC cell lines were gifts from Dr. Xue-Ru Wu (Departments of Urology and Pathology, New York University School of Medicine, New York, NY, USA). Cell transfections were performed with PolyJet DNA In Vitro Transfection Reagent (SignaGen Laboratories, Rockville, MD, USA) according to the manufacturer's instructions. For stable transfection, cell cultures were subjected to selection with hygromycin B (200–400 μg/mL), G418 (500–1000 μg/mL), or puromycin (0.2–0.3 μg/mL), depending on the different antibiotic resistance plasmids transfected. Cells surviving antibiotic selections were pooled as stable mass transfectants, as described in previous studies.[68]

Western Blot

Cells were extracted with cell lysis buffer (10 mM Tris-HCl [pH 7.4], 1% SDS, and 1 mM Na_3VO_4) using standard protocols. Protein concentrations in the lysates were then determined using a NanoDrop 2000 spectrophotometer (Thermo Scientific, Waltham, MA, USA). Aliquots (containing 100 μg protein) of each cell extract were then subjected to SDS-PAGE and were then electrotransferred to polyvinylidene fluoride membranes (Bio-Rad, Hercules, CA, USA). Any protein that specifically bound corresponding primary antibody was detected using an alkaline-phosphatase-linked secondary antibody followed by treatment to enhance chemifluorescence. All blot images were then captured by using a Typhoon FLA 7000 system (GE Healthcare, Chicago, IL, USA).

Luciferase Reporter Assay

The cells were transfected with the indicated luciferase reporter in combination with the pRL-TK vector (Promega, Fitchburg, WI, USA) as an internal control. Luciferase activities were determined using a microplate luminometer, as described earlier.[69]

Human BC Tissues

A total of 23 pairs of primary invasive BC samples and their paired adjacent normal bladder tissues were obtained from patients who underwent radical cystectomy at the Department of Urology of the Union Hospital (Tongji Medical College, Wuhan, China) between 2012 and 2013. All specimens were immediately snap frozen in liquid nitrogen after surgical resection. All specimens were obtained with appropriate informed consent from the patients and a supportive grant obtained from the Medical Ethics Committee of China.

Confocal Laser Scanning Microscopy

Cells with mcherry-LC3 were seeded onto chamber slides (10^4 per well) in a 1:1 mixture of DMEM/Ham's F12 medium supplemented with 5% fetal bovine serum (FBS) and cultured at 37°C in a 5% CO_2 incubator. When cell density reached an optimal 70%–80% confluency, the cells were then treated with 8 μM ChlA-F and incubated for varying lengths of time. At each time point, slides containing the cells were removed, washed with pre-warmed PBS once, then fixed in 4% paraformaldehyde for 30 min at room temperature. The slides were then washed twice with pre-warmed PBS, and the cells on the membrane were permeabilized with PBS containing 0.2% Triton X-100 (15 min, room temperature). After staining with DAPI (0.1 mg/mL) (Sigma, 9542) for 30 min, the slides were washed three times with PBS and coated with anti-fade reagent (Molecular Probes, P36930, Eugene, OR, USA). Cellular images were then captured using an inverted Leica fluorescence microscope (Wetzlar, Germany). Cells with ≥ 5 intense mcherry-LC3 puncta were considered autophagic cells, whereas those with diffuse cytoplasmic mcherry-LC3 staining were considered non-autophagic cells. The percentages of the mcherry-LC3-positive cells were calculated based on at least 200 counted cells. The number of mcherry-LC3 puncta per cell was counted for at least 50 cells.

In Vitro Cellular Migration and Invasion Assays

In vitro migration and invasion assays were conducted using Transwell chambers (for migration assay) or Transwell pre-coated Matrigel chambers (for invasion assay), according to manufacturer protocols (BD Biosciences, Bedford, MA) (26, 27). In brief, 700 μL medium containing 10% FBS (for UMUC6 and U5637 cells) was added to the lower chambers, while homogeneous single-cell suspensions (5×10^4 cells per well) in 0.1% FBS medium were added to the upper chambers. Then, the plates were incubated in a 5% CO_2 incubator at 37°C for 24 h, wells were washed using PBS, and well contents were fixed (4% formaldehyde) and stained (Giemsa). Non-migrating or

non-invading cells were scraped off. Migration and invasion rates were then quantified by counting migrating and invading cells in at least three random fields under a light microscope (Olympus, Center Valley, PA, USA).[70]

RIP

Cells were cultured in 10-cm dishes and harvested by scraping after each specific treatment. Polysome lysis buffer (PLB) containing 10 mm HEPES (pH 7), 100 mM KCl, 5 mM $MgCl_2$, 25 mM EDTA, 0.5% (v/v) IGEPAL, 2 mM dithiothreitol (DTT), RNase OUT (50 U/mL), Superase IN (50 U/mL), heparin (0.2 mg/mL), and complete proteinase inhibitor was used to lyse each cell pellet. The resulting lysate was centrifuged (14,000 × *g*, 10 min, 4°C), and the supernatant was recovered. Anti-PP2A-c antibody and protein A/G agarose beads were added to the supernatant, and the suspension was rotated overnight at 4°C in NET2 buffer containing 50 mm Tris-HCl (pH 7.4), 150 mM NaCl, 1 mM $MgCl_2$, 0.05% (v/v) IGEPAL, RNase OUT (50 U/mL), Superase IN (50 U/mL), 1 mM DTT, and 30 mM EDTA. The beads were washed three times, re-suspended in 100 μL NET2 and 100 μL SDS-TE (20 mm Tris-HCl [pH 7.5], 2 mM EDTA, 2% SDS), and then incubated for 30 min at 55°C, with occasional mixing. All RNAs in the buffer were extracted using phenol-chloroform-isoamyl alcohol, and qPCR was then performed (discussed later) to detect SNHG1 presented in the immune complex.

Quantitative Real-Time PCR

Total RNA was extracted with TRIzol reagent (Invitrogen, Carlsbad, CA, USA) according to the manufacturer's instructions. Specific cDNA was then synthesized with the ThermoScript RT-PCR System (Invitrogen). A pair of oligonucleotides (forward [F], 5′-GATGAT CTT GAGGCTGTTGTC-3′; and reverse [R], 5′-CAGGGCTGCTTT TAACTCTG-3′) were used to amplify human *GAPDH* cDNA as the loading control. The human *SNHG1* cDNA fragments were amplified using the following primers: F, 5′-AGCAGACACAGATTAA GACA-3′; and R, 5′-GGCAGGTAGATTCCAGATAA-3′. Human *MMP2* cDNA fragments were amplified using the following primers: F, 5′-CAAGTGGGACAAGAA CCAGA-3′; and R, 5′-CC AAAGTTGATCATGATGTC-3′. Human *PP2A-c* cDNA fragments were amplified using the following primers: F, 5′-TTGATCGCCTA CAAGAAGTTCCCCA-3′; and R, 5′-CTCTACGAGGTGCTGGG TCAAACTG-3′.

Total miRNA was extracted using a miRNeasy Mini Kit (QIAGEN, Valencia, CA, USA). Reverse transcription was then performed using a miScript II RT Kit (QIAGEN), and quantitative real-time PCR was performed using the miScript PCR Starter Kit (QIAGEN), in both cases according to the manufacturer's protocols. U6 was used as the endogenous normalizer. Cycle threshold (C_t) values were determined, and relative expression of each miRNA was calculated using the values of $2^{-\Delta\Delta Ct}$.

Co-immunoprecipitation (co-IP) Assay

U5637(Vector) and U5637(SNHG1) cells were cultured in 10-cm dishes until cell concentrations reached 70%–80%. Culture medium was then removed and replaced by DMEM containing 0.1% FBS for 12 h. The cells were then collected and lysed in Cell Lysis Buffer (Cell Signaling Technology) containing protease inhibitors (Roche, Branchburg, NJ, USA) and briefly sonicated. The extracts were then incubated overnight at 4°C with anti-PP2A-c or anti-rabbit IgG (immunoglobulin G) (Cell Signaling Technology) with protein A/G agarose beads. The beads were then washed three times with Cell Lysis Buffer, and bound proteins were eluted using 2× SDS sample buffer (Cell Signaling Technology, Beverly, MA, USA). Eluted proteins were then quantified by the Lowry protein assay, and aliquots were then subjected to western blot assays.

Statistical Analysis

Statistical analyses were performed using SPSS v.19.0 software (SPSS, Chicago, IL, USA). A Student's t test or ANOVA was used to determine significant differences between the outcomes of two groups/time points in all cases; $p < 0.05$ was considered significant.

Ethics Approval and Consent to Participate

All specimens were obtained with appropriate informed consent from the patients. Human studies were approved by the Medical Ethics Committee of the Union Hospital of Tongji Medical College (Wuhan, China). The experiments were carried out in accordance with the Code of Ethics of the World Medical Association (Declaration of Helsinki) for experiments involving human studies.

AUTHOR CONTRIBUTIONS

C.H. and J.X. designed the study. R.Y. and X.H. detected the cells' biological function, conducted the real-time PCR assays, carried out the western blot assays and Luciferase reporter assays, and performed the statistical analysis. J.X. drafted the manuscript. M.H., Z.T., J.L., H.Y.L., G.J., and M.C. helped to acquire the experimental data. All authors read and approved the final manuscript.

CONFLICTS OF INTEREST

The authors declare no competing interests.

ACKNOWLEDGMENTS

The authors sincerely thank Dr. Gang Chen (University of Kentucky, Lexington, KY, USA) for providing the GFP-LC3 construct. This work was partially supported by grants of the United States NCI CA177665, CA165989, and NIEHS ES000260.

REFERENCES

1. Bray, F., Ferlay, J., Soerjomataram, I., Siegel, R.L., Torre, L.A., and Jemal, A. (2018). Global cancer statistics 2018: GLOBOCAN estimates of incidence and mortality worldwide for 36 cancers in 185 countries. CA Cancer J. Clin. *68*, 394–424.

2. Saginala, K., Barsouk, A., Aluru, J.S., Rawla, P., Padala, S.A., and Barsouk, A. (2020). Epidemiology of Bladder Cancer. Med. Sci. (Basel) *8*, 15.

3. Chou, R., Selph, S.S., Buckley, D.I., Gustafson, K.S., Griffin, J.C., Grusing, S.E., and Gore, J.L. (2016). Treatment of muscle-invasive bladder cancer: A systematic review. Cancer *122*, 842–851.

4. Choi, W., Czerniak, B., Ochoa, A., Su, X., Siefker-Radtke, A., Dinney, C., and McConkey, D.J. (2014). Intrinsic basal and luminal subtypes of muscle-invasive bladder cancer. Nat. Rev. Urol. *11*, 400–410.

5. Sjodahl, G., Eriksson, P., Lovgren, K., Marzouka, N.A., Bernardo, C., Nordentoft, I., Dyrskjøt, L., Liedberg, F., and Höglund, M. (2018). Discordant molecular subtype classification in the basal-squamous subtype of bladder tumors and matched lymph-node metastases. Mod. Pathol. *31*, 1869–1881.

6. Dadhania, V., Zhang, M., Zhang, L., Bondaruk, J., Majewski, T., Siefker-Radtke, A., Guo, C.C., Dinney, C., Cogdell, D.E., Zhang, S., et al. (2016). Meta-Analysis of the Luminal and Basal Subtypes of Bladder Cancer and the Identification of Signature Immunohistochemical Markers for Clinical Use. EBioMedicine *12*, 105–117.

7. Choi, W., Porten, S., Kim, S., Willis, D., Plimack, E.R., Hoffman-Censits, J., Roth, B., Cheng, T., Tran, M., Lee, I.L., et al. (2014). Identification of distinct basal and luminal subtypes of muscle-invasive bladder cancer with different sensitivities to frontline chemotherapy. Cancer Cell *25*, 152–165.

8. Robertson, A.G., Kim, J., Al-Ahmadie, H., Bellmunt, J., Guo, G., Cherniack, A.D., Hinoue, T., Laird, P.W., Hoadley, K.A., Akbani, R., et al. (2017). Comprehensive Molecular Characterization of Muscle-Invasive Bladder Cancer. Cell *171*, 540–556.e25.

9. Liu, G., Chen, Z., Danilova, I.G., Bolkov, M.A., Tuzankina, I.A., and Liu, G. (2018). Identification of miR-200c and miR141-Mediated lncRNA-mRNA Crosstalks in Muscle-Invasive Bladder Cancer Subtypes. Front. Genet. *9*, 422.

10. Taheri, M., Habibi, M., Noroozi, R., Rakhshan, A., Sarrafzadeh, S., Sayad, A., Omrani, M.D., and Ghafouri-Fard, S. (2017). HOTAIR genetic variants are associated with prostate cancer and benign prostate hyperplasia in an Iranian population. Gene *613*, 20–24.

11. Nikpayam, E., Tasharrofi, B., Sarrafzadeh, S., and Ghafouri-Fard, S. (2017). The Role of Long Non-Coding RNAs in Ovarian Cancer. Iran. Biomed. J. *21*, 3–15.

12. Luo, J., Chen, J., Li, H., Yang, Y., Yun, H., Yang, S., and Mao, X. (2017). LncRNA UCA1 promotes the invasion and EMT of bladder cancer cells by regulating the miR-143/HMGB1 pathway. Oncol. Lett. *14*, 5556–5562.

13. Qin, Z., Wang, Y., Tang, J., Zhang, L., Li, R., Xue, J., Han, P., Wang, W., Qin, C., Xing, Q., et al. (2018). High LINC01605 expression predicts poor prognosis and promotes tumor progression via up-regulation of MMP9 in bladder cancer. Biosci. Rep. *38*, BSR20180562.

14. Sun, Y., Liu, J., Chu, L., Yang, W., Liu, H., Li, C., and Yang, J. (2018). Long noncoding RNA SNHG12 facilitates the tumorigenesis of glioma through miR-101-3p/FOXP1 axis. Gene *676*, 315–321.

15. Zhang, Y., Jin, X., Wang, Z., Zhang, X., Liu, S., and Liu, G. (2017). Downregulation of SNHG1 suppresses cell proliferation and invasion by regulating Notch signaling pathway in esophageal squamous cell cancer. Cancer Biomark. *21*, 89–96.

16. Hu, Y., Ma, Z., He, Y., Liu, W., Su, Y., and Tang, Z. (2017). LncRNA-SNHG1 contributes to gastric cancer cell proliferation by regulating DNMT1. Biochem. Biophys. Res. Commun. *491*, 926–931.

17. Zhang, Y., Zhang, R., Luo, G., and Ai, K. (2018). Long noncoding RNA SNHG1 promotes cell proliferation through PI3K/AKT signaling pathway in pancreatic ductal adenocarcinoma. J. Cancer *9*, 2713–2722.

18. Cui, L., Dong, Y., Wang, X., Zhao, X., Kong, C., Liu, Y., Jiang, X., and Zhang, X. (2019). Downregulation of long noncoding RNA SNHG1 inhibits cell proliferation, metastasis, and invasion by suppressing the Notch-1 signaling pathway in pancreatic cancer. J. Cell. Biochem. *120*, 6106–6112.

19. Zhang, S., and Song, X. (2019). Long non-coding RNA SNHG1 promotes cell proliferation and invasion of hepatocellular carcinoma by acting as a molecular sponge to modulate miR-195. Arch. Med. Sci. *16*, 386–394.

20. Mobley, A., Zhang, S.Z., Bondaruk, J., Wang, Y., Majewski, T., Caraway, N.P., Huang, L., Shoshan, E., Velazquez-Torres, G., Nitti, G., et al. (2017). Aurora Kinase A is a Biomarker for Bladder Cancer Detection and Contributes to its Aggressive Behavior. Sci. Rep. *7*, 40714.

21. Yang, R., Xu, J., Hua, X., Tian, Z., Xie, Q., Li, J., Jiang, G., Cohen, M., Sun, H., and Huang, C. (2020). Overexpressed miR-200a promotes bladder cancer invasion through direct regulating Dicer/miR-16/JNK2/MMP-2 axis. Oncogene *39*, 1983–1996.

22. Jin, H., Yu, Y., Hu, Y., Lu, C., Li, J., Gu, J., Zhang, L., Huang, H., Zhang, D., Wu, X.R., et al. (2015). Divergent behaviors and underlying mechanisms of cell migration and invasion in non-metastatic T24 and its metastatic derivative T24T bladder cancer cell lines. Oncotarget *6*, 522–536.

23. van Zijl, F., Krupitza, G., and Mikulits, W. (2011). Initial steps of metastasis: cell invasion and endothelial transmigration. Mutat. Res. *728*, 23–34.

24. Zhu, J., Xu, C., Ruan, L., Wu, J., Li, Y., and Zhang, X. (2019). MicroRNA-146b Overexpression Promotes Human Bladder Cancer Invasion via Enhancing ETS2-Mediated mmp2 mRNA Transcription. Mol. Ther. Nucleic Acids *16*, 531–542.

25. Bindhu, O.S., Ramadas, K., Sebastian, P., and Pillai, M.R. (2006). High expression levels of nuclear factor kappa B and gelatinases in the tumorigenesis of oral squamous cell carcinoma. Head Neck *28*, 916–925.

26. Deng, R., Mo, F., Chang, B., Zhang, Q., Ran, H., Yang, S., Zhu, Z., Hu, L., and Su, Q. (2017). Glucose-derived AGEs enhance human gastric cancer metastasis through RAGE/ERK/Sp1/MMP2 cascade. Oncotarget *8*, 104216–104226.

27. Fromigué, O., Hamidouche, Z., and Marie, P.J. (2008). Blockade of the RhoA-JNK-c-Jun-MMP2 cascade by atorvastatin reduces osteosarcoma cell invasion. J. Biol. Chem. *283*, 30549–30556.

28. Al-Murrani, S.W.K., Woodgett, J.R., and Damuni, Z. (1999). Expression of I2PP2A, an inhibitor of protein phosphatase 2A, induces c-Jun and AP-1 activity. Biochem. J. *341*, 293–298.

29. Cao, Z., Zhang, R., Li, J., Huang, H., Zhang, D., Zhang, J., Gao, J., Chen, J., and Huang, C. (2013). X-linked inhibitor of apoptosis protein (XIAP) regulation of cyclin D1 protein expression and cancer cell anchorage-independent growth via its E3 ligase-mediated protein phosphatase 2A/c-Jun axis. J. Biol. Chem. *288*, 20238–20247.

30. Chou, C.H., Chang, N.W., Shrestha, S., Hsu, S.D., Lin, Y.L., Lee, W.H., Yang, C.D., Hong, H.C., Wei, T.Y., Tu, S.J., et al. (2016). miRTarBase 2016: updates to the experimentally validated miRNA-target interactions database. Nucleic Acids Res. *44* (D1), D239–D247.

31. Gibbings, D., Mostowy, S., and Voinnet, O. (2013). Autophagy selectively regulates miRNA homeostasis. Autophagy *9*, 781–783.

32. Peng, M., Wang, J., Tian, Z., Zhang, D., Jin, H., Liu, C., Xu, J., Li, J., Hua, X., Xu, J., et al. (2019). Autophagy-mediated *Mir6981* degradation exhibits *CDKN1B* promotion of PHLPP1 protein translation. Autophagy *15*, 1523–1538.

33. Knowles, M.A., and Hurst, C.D. (2015). Molecular biology of bladder cancer: new insights into pathogenesis and clinical diversity. Nat. Rev. Cancer *15*, 25–41.

34. Xu, W., Xia, H., Liu, W., Zheng, W., and Hua, L. (2018). Exploration of genetics commonness between bladder cancer and breast cancer based on a silcio analysis on disease subtypes. Technol. Health Care *26* (S1), 361–377.

35. Volkmer, J.P., Sahoo, D., Chin, R.K., Ho, P.L., Tang, C., Kurtova, A.V., Willingham, S.B., Pazhanisamy, S.K., Contreras-Trujillo, H., Storm, T.A., et al. (2012). Three differentiation states risk-stratify bladder cancer into distinct subtypes. Proc. Natl. Acad. Sci. USA *109*, 2078–2083.

36. Chandrasekar, T., Erlich, A., and Zlotta, A.R. (2018). Molecular Characterization of Bladder Cancer. Curr. Urol. Rep. *19*, 107.

37. Sjödahl, G., Lövgren, K., Lauss, M., Patschan, O., Gudjonsson, S., Chebil, G., Aine, M., Eriksson, P., Månsson, W., Lindgren, D., et al. (2013). Toward a molecular pathologic classification of urothelial carcinoma. Am. J. Pathol. *183*, 681–691.

38. Mai, K.T., Truong, L.D., Ball, C.G., Williams, P., Flood, T.A., and Belanger, E.C. (2015). Invasive urothelial carcinoma exhibiting basal cell immunohistochemical markers: A variant of urothelial carcinoma associated with aggressive features. Pathol. Res. Pract. *211*, 610–618.

39. Sullenger, B.A., and Nair, S. (2016). From the RNA world to the clinic. Science *352*, 1417–1420.

40. Schmitt, A.M., and Chang, H.Y. (2016). Long Noncoding RNAs in Cancer Pathways. Cancer Cell *29*, 452–463.

41. Schmitz, S.U., Grote, P., and Herrmann, B.G. (2016). Mechanisms of long noncoding RNA function in development and disease. Cell. Mol. Life Sci. *73*, 2491–2509.

42. Esteller, M. (2011). Non-coding RNAs in human disease. Nat. Rev. Genet. *12*, 861–874.

43. Zhou, C., Huang, C., Wang, J., Huang, H., Li, J., Xie, Q., Liu, Y., Zhu, J., Li, Y., Zhang, D., et al. (2017). LncRNA MEG3 downregulation mediated by DNMT3b contributes to nickel malignant transformation of human bronchial epithelial cells via modulating PHLPP1 transcription and HIF-1α translation. Oncogene *36*, 3878–3889.

44. Zhang, M., Wang, W., Li, T., Yu, X., Zhu, Y., Ding, F., Li, D., and Yang, T. (2016). Long noncoding RNA SNHG1 predicts a poor prognosis and promotes hepatocellular carcinoma tumorigenesis. Biomed. Pharmacother. *80*, 73–79.

45. Zhang, H., Zhou, D., Ying, M., Chen, M., Chen, P., Chen, Z., and Zhang, F. (2016). Expression of Long Non-Coding RNA (lncRNA) Small Nucleolar RNA Host Gene 1 (SNHG1) Exacerbates Hepatocellular Carcinoma Through Suppressing miR-195. Med. Sci. Monit. *22*, 4820–4829.

46. You, J., Fang, N., Gu, J., Zhang, Y., Li, X., Zu, L., and Zhou, Q. (2014). Noncoding RNA small nucleolar RNA host gene 1 promote cell proliferation in nonsmall cell lung cancer. Indian J. Cancer *51* (*Suppl. 3*), e99–e102.

47. Li, J., Zhang, Z., Xiong, L., Guo, C., Jiang, T., Zeng, L., Li, G., and Wang, J. (2017). SNHG1 lncRNA negatively regulates miR-199a-3p to enhance CDK7 expression and promote cell proliferation in prostate cancer. Biochem. Biophys. Res. Commun. *487*, 146–152.

48. Zhu, J., Tian, Z., Li, Y., Hua, X., Zhang, D., Li, J., Jin, H., Xu, J., Chen, W., Niu, B., et al. (2019). ATG7 Promotes Bladder Cancer Invasion via Autophagy-Mediated Increased ARHGDIB mRNA Stability. Adv. Sci. (Weinh.) *6*, 1801927.

49. Zhu, J., Li, Y., Tian, Z., Hua, X., Gu, J., Li, J., Liu, C., Jin, H., Wang, Y., Jiang, G., et al. (2017). ATG7 Overexpression Is Crucial for Tumorigenic Growth of Bladder Cancer In Vitro and In Vivo by Targeting the ETS2/miRNA196b/FOXO1/p27 Axis. Mol. Ther. Nucleic Acids *7*, 299–313.

50. Wong, S.Y., and Kumar, S. (2014). Matrix regulation of tumor-initiating cells. Prog. Mol. Biol. Transl. Sci. *126*, 243–256.

51. Chen, J.S., Huang, X.H., Wang, Q., Huang, J.Q., Zhang, L.J., Chen, X.L., Lei, J., and Cheng, Z.X. (2013). Sonic hedgehog signaling pathway induces cell migration and invasion through focal adhesion kinase/AKT signaling-mediated activation of matrix metalloproteinase (MMP)-2 and MMP-9 in liver cancer. Carcinogenesis *34*, 10–19.

52. Stamenkovic, I. (2000). Matrix metalloproteinases in tumor invasion and metastasis. Semin. Cancer Biol. *10*, 415–433.

53. Tao, L., Li, Z., Lin, L., Lei, Y., Hongyuan, Y., Hongwei, J., Yang, L., and Chuize, K. (2015). MMP1, 2, 3, 7, and 9 gene polymorphisms and urinary cancer risk: a meta-analysis. Genet. Test. Mol. Biomarkers *19*, 548–555.

54. Peng, M., Wang, J., Zhang, D., Jin, H., Li, J., Wu, X.R., and Huang, C. (2018). PHLPP2 stabilization by p27 mediates its inhibition of bladder cancer invasion by promoting autophagic degradation of MMP2 protein. Oncogene *37*, 5735–5748.

55. Huang, H., Jin, H., Zhao, H., Wang, J., Li, X., Yan, H., Wang, S., Guo, X., Xue, L., Li, J., et al. (2017). RhoGDIβ promotes Sp1/MMP-2 expression and bladder cancer invasion through perturbing miR-200c-targeted JNK2 protein translation. Mol. Oncol. *11*, 1579–1594.

56. Jiang, G., Wu, A.D., Huang, C., Gu, J., Zhang, L., Huang, H., Liao, X., Li, J., Zhang, D., Zeng, X., et al. (2016). Isorhapontigenin (ISO) Inhibits Invasive Bladder Cancer Formation In Vivo and Human Bladder Cancer Invasion In Vitro by Targeting STAT1/FOXO1 Axis. Cancer Prev. Res. (Phila.) *9*, 567–580.

57. Xu, J., Hua, X., Yang, R., Jin, H., Li, J., Zhu, J., Tian, Z., Huang, M., Jiang, G., Huang, H., and Huang, C. (2019). XIAP Interaction with E2F1 and Sp1 via its BIR2 and BIR3 domains specific activated MMP2 to promote bladder cancer invasion. Oncogenesis *8*, 71.

58. Winerdal, M.E., Krantz, D., Hartana, C.A., Zirakzadeh, A.A., Linton, L., Bergman, E.A., Rosenblatt, R., Vasko, J., Alamdari, F., Hansson, J., et al. (2018). Urinary Bladder Cancer Tregs Suppress MMP2 and Potentially Regulate Invasiveness. Cancer Immunol. Res. *6*, 528–538.

59. Shimada, K., Nakamura, M., Ishida, E., Higuchi, T., Tanaka, M., Ota, I., and Konishi, N. (2007). c-Jun NH2 terminal kinase activation and decreased expression of mitogen-activated protein kinase phosphatase-1 play important roles in invasion and angiogenesis of urothelial carcinomas. Am. J. Pathol. *171*, 1003–1012.

60. Mazhar, S., Taylor, S.E., Sangodkar, J., and Narla, G. (2019). Targeting PP2A in cancer: Combination therapies. Biochim. Biophys. Acta Mol. Cell Res. *1866*, 51–63.

61. Hua, X., Xu, J., Deng, X., Xu, J., Li, J., Zhu, D.Q., Zhu, J., Jin, H., Tian, Z., Huang, H., et al. (2018). New compound ChlA-F induces autophagy-dependent anti-cancer effect via upregulating Sestrin-2 in human bladder cancer. Cancer Lett. *436*, 38–51.

62. Guo, X., Huang, H., Jin, H., Xu, J., Risal, S., Li, J., Li, X., Yan, H., Zeng, X., Xue, L., et al. (2018). ISO, via Upregulating MiR-137 Transcription, Inhibits GSK3β-HSP70-MMP-2 Axis, Resulting in Attenuating Urothelial Cancer Invasion. Mol. Ther. Nucleic Acids *12*, 337–349.

63. Xie, F., Li, Y., Wang, M., Huang, C., Tao, D., Zheng, F., Zhang, H., Zeng, F., Xiao, X., and Jiang, G. (2018). Circular RNA BCRC-3 suppresses bladder cancer proliferation through miR-182-5p/p27 axis. Mol. Cancer *17*, 144.

64. Su, Y., Lu, S., Li, J., and Deng, L. (2018). Shikonin-mediated up-regulation of miR-34a and miR-202 inhibits retinoblastoma proliferation. Toxicol. Res. (Camb.) *7*, 907–912.

65. Toraih, E.A., Ibrahiem, A.T., Fawzy, M.S., Hussein, M.H., Al-Qahtani, S.A.M., and Shaalan, A.A.M. (2017). MicroRNA-34a: A Key Regulator in the Hallmarks of Renal Cell Carcinoma. Oxid. Cell. Med. Longev. *2017*, 3269379.

66. Wang, A.M., Huang, T.T., Hsu, K.W., Huang, K.H., Fang, W.L., Yang, M.H., Lo, S.S., Chi, C.W., Lin, J.J., and Yeh, T.S. (2014). Yin Yang 1 is a target of microRNA-34 family and contributes to gastric carcinogenesis. Oncotarget *5*, 5002–5016.

67. Wiggins, J.F., Ruffino, L., Kelnar, K., Omotola, M., Patrawala, L., Brown, D., and Bader, A.G. (2010). Development of a lung cancer therapeutic based on the tumor suppressor microRNA-34. Cancer Res. *70*, 5923–5930.

68. Zhu, J., Li, Y., Chen, C., Ma, J., Sun, W., Tian, Z., Li, J., Xu, J., Liu, C.S., Zhang, D., et al. (2017). NF-κB p65 Overexpression Promotes Bladder Cancer Cell Migration via FBW7-Mediated Degradation of RhoGDIα Protein. Neoplasia *19*, 672–683.

69. Yu, Y., Jin, H., Xu, J., Gu, J., Li, X., Xie, Q., Huang, H., Li, J., Tian, Z., Jiang, G., et al. (2018). XIAP overexpression promotes bladder cancer invasion in vitro and lung metastasis in vivo via enhancing nucleolin-mediated Rho-GDIβ mRNA stability. Int. J. Cancer *142*, 2040–2055.

70. Jin, H., Xie, Q., Guo, X., Xu, J., Wang, A., Li, J., Zhu, J., Wu, X.R., Huang, H., and Huang, C. (2017). p63α protein up-regulates heat shock protein 70 expression via E2F1 transcription factor 1, promoting Wasf3/Wave3/MMP9 signaling and bladder cancer invasion. J. Biol. Chem. *292*, 15952–15963.